


## ORIGINAL RESEARCH PAPER

# Study on the residual flux density measurement method for power transformer cores based on magnetising inductance

Cailing Huo<sup>1</sup>  | Youhua Wang<sup>1</sup> | Chengcheng Liu<sup>1</sup> | Gang Lei<sup>2</sup>

<sup>1</sup>State Key Laboratory of Reliability and Intelligence of Electrical Equipment, Hebei University of Technology, Tianjin, China

<sup>2</sup>Electrical Department, School of Electrical and Data Engineering, University of Technology Sydney, Sydney, New South Wales, Australia

## Correspondence

Youhua Wang, State Key Laboratory of Reliability and Intelligence of Electrical Equipment, Hebei University of Technology, Tianjin 300130, China.  
Email: wangyh@hebut.edu.cn

## Funding information

National Natural Science Foundation of China, Grant/Award Number: 51877065; Science and Technology Research Project of Higher Education Institutions in Hebei Province of China, Grant/Award Number: QN2016200

## Abstract

When a power transformer is reconnected to a power grid, if the residual flux in its iron core is large, significant inrush current may be generated and result in closing failure. Therefore, accurate residual flux measurement is necessary to avoid the harmful effects of inrush current. This work proposes a residual flux density measurement method for the power transformer core based on magnetising inductance. Firstly, when positive and negative DC voltages are applied along or opposite to the direction of the initial residual flux density, the measured positive magnetising inductance is smaller than the negative so that the direction of residual flux density can be determined by comparing their values. Secondly, the magnitude of residual flux density can be calculated by analysing the empirical formula between residual flux density and positive magnetising inductance using the finite element method. Finally, this work takes the square iron core as the research object, establishes the corresponding empirical formula, and verifies its accuracy through experiments. The experimental results show that the proposed method has higher accuracy compared with the voltage integration method widely used in this field.

## KEYWORDS

power system simulation, power transformers

## 1 | INTRODUCTION

When a power transformer is powered off, due to the hysteresis characteristics of ferromagnetic materials, there is a residual flux density ( $B_r$ ) in its iron core [1]. If the residual flux is large, significant inrush current may be generated, and its magnitude may reach 6–8 times the rated current. This leads to failure in reclosing the transformer, which is not conducive to the safe operation of the power grid [2]. To overcome this issue, DC demagnetisation operation can be performed to the iron core [3]. However, due to the unknown residual flux, it requires multiple demagnetizations to completely eliminate the residual flux [4]. If the residual flux can be accurately measured, the DC demagnetisation excitation can be determined, which will reduce the adverse effects on the transformer caused by repeated operations in direct demagnetisation. Therefore, accurate residual flux detection is of great significance for reducing inrush current.

The empirical estimation method is generally used to estimate residual flux in the iron core [5]. The residual flux is estimated to be 20%–70% of the saturation flux [6, 7].

However, the estimation error may be large as this method depends on historical experience. Another method is the voltage integration method. After a transformer is powered off, it can be employed to integrate the induced voltage waveform of winding to obtain a steady-state magnetic flux, which is the residual flux [8]. This method is currently the most widely used method for measuring changes in magnetic flux. Nevertheless, due to hysteresis characteristics of the ferromagnetic material, the calculated residual flux at the time of opening is different from the residual flux after stabilisation, and thus the feasibility of this method is limited. Moreover, a pre-magnetization method has been proposed on the basis of a known residual flux [9–11]. When positive and negative DC voltages are applied, the residual flux and residual flux coefficient can be estimated by measuring the magnetic flux at the saturation point and the current crossing zero point. However, after the transformer is powered off, the direction of residual flux is unknown and the magnetization direction of the core cannot be judged. Thus, this method cannot be applied to actual transformer cores.

This is an open access article under the terms of the Creative Commons Attribution-NonCommercial-NoDerivs License, which permits use and distribution in any medium, provided the original work is properly cited, the use is non-commercial and no modifications or adaptations are made.

© 2021 The Authors. *IET Electric Power Applications* published by John Wiley & Sons Ltd on behalf of The Institution of Engineering and Technology.

Since the generation of residual flux involves complex magnetic domain structure changes [12, 13], the residual flux cannot be measured directly. In Refs. [14–16], the residual flux is measured by controlling the closing angle and analysis inrush current. This method can measure a certain range of residual flux, but when the residual flux is large, the measurement error may be greater than that in the voltage integration method. In Ref. [17], the residual flux in the current transformer (CT) is calculated by considering the relationship between the residual flux and the even harmonics of the induced voltage. This method can quickly and effectively detect the residual flux of CT, but its measurement accuracy is mainly dependent on the simulation model. Thus, whether this method can be applied to the actual transformer core needs further verification. In Ref. [18], the residual flux is measured by a transfer function of leakage flux and residual flux. This method is conducive to on-site measurement of transformers. However, as different measurement points have different transfer functions, the measurement accuracy greatly is affected by the measurement points. In Ref. [19], the residual flux is obtained by actually measuring the energy of the minor hysteresis loops. In this method, when the residual flux is small, the energy change is not much different under different residual fluxes, which makes the measurement error larger. This method also cannot determine the direction of the residual flux. When the DC voltage is loaded, the residual flux is calculated by analysing the relationship between residual flux and transient characteristics. In Refs. [20, 21], the residual flux density is measured by the transient current when the DC voltage is applied. This method uses the finite element method (FEM) to obtain the empirical formula for calculating the residual flux, so the measurement results depend entirely on the accuracy of the finite element model. In FEM, the material properties of the transformer core are used to replace the local magnetic properties at residual flux, which reduces the accuracy of the established finite element model. In addition, it is more troublesome to select the measurement time of transient current in this method, and different measurement times have different empirical formulas. Therefore, there is no effective method for measuring residual flux density in the iron core.

This work presents a residual flux density measurement method for power transformer cores based on magnetising inductance. The proposed method mainly has the following improvements:

- (1) To overcome the inaccuracy of the finite element model, local magnetic properties are measured in this study
- (2) The magnetising inductance is used as the independent variable to measure the residual flux, which avoids the error caused by the inaccurate selection of transient current in the above method
- (3) When positive and negative DC voltages are applied, the direction of residual flux density can be judged by comparing the values of the positive and negative magnetising inductances
- (4) The empirical formula for calculating the residual flux density is obtained by FEM and its accuracy is verified on the

experimental platform. The results show that the measurement error of the proposed method is less than 5%, which has a higher accuracy than the voltage integration method

- (5) The range of applied DC voltage is determined. In this range, the residual flux density changes very little, which improves the applicability of the empirical formula in the experiment

The rest of the work is organised as follows: Section 2 presents the principle of the proposed measurement method. Section 3 obtains the proposed empirical formula for calculating the residual flux density by using FEM. In Section 4, an experimental platform for the proposed method is established, and the accuracy of the proposed method is verified. Section 5 concludes the pros and cons of the proposed method and discusses future research work.

## 2 | PRINCIPLE OF PROPOSED MEASUREMENT METHOD

### 2.1 | Generation principle of residual flux density

Figure 1 shows the generation principle of  $B_r$  and the magnetic domain structure changes during the magnetization process. As shown, the magnetization process is divided into the following: (1) Initial state. At this time, the magnetic domains inside the iron core are arranged in a disorderly manner, and thus the iron core does not show magnetism to the outside. (2) Reversible magnetization state: When the magnetic field strength ( $H$ ) increases from 0 to point  $a$ , the reversible magnetic domain wall displacement between magnetic domains is generated. At this time, if  $H$  disappears, there is almost no  $B_r$  in the iron core. (3) Irreversible magnetization state: As  $H$  continues to increase to point  $b$ , the magnetic domain movement begins to change from reversible to irreversible magnetic domain wall displacement, showing strong magnetism to the outside. After  $H$  disappears, the magnetic domain cannot return to its original state and produces a  $B_r$ . (4) Saturation magnetization state: When  $H$  continues to increase to point  $c$ , the iron core enters the saturation state and thus the ability of magnetic domain to be magnetised is weakened. After  $H$  is removed, a large  $B_r$  is produced in the iron core. This phenomenon is called the hysteresis characteristic of ferromagnetic materials. Due to this characteristic,  $B_r$  is mainly related to the change of magnetic domains from point  $b$  or  $c$  to the  $B_r$  state. This change can be reflected by the relative differential permeability ( $\mu_{rd}$ ), which is defined as the incremental ratio of magnetic flux density ( $\Delta B_r$ ) and magnetic field strength ( $\Delta H$ ) at  $B_r$ .

$$\mu_{rd} = \frac{1}{\mu_0} \frac{\Delta B_r}{\Delta H} \quad (1)$$

where  $\mu_0$  expresses the permeability of air, and its value is  $4\pi \times 10^{-7}$  H/m.

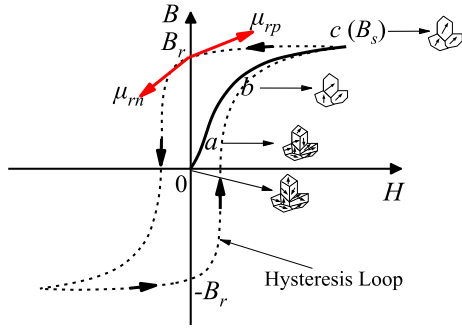


**FIGURE 1** Generation principle of residual flux density and the magnetic domain structure changes during the magnetization process

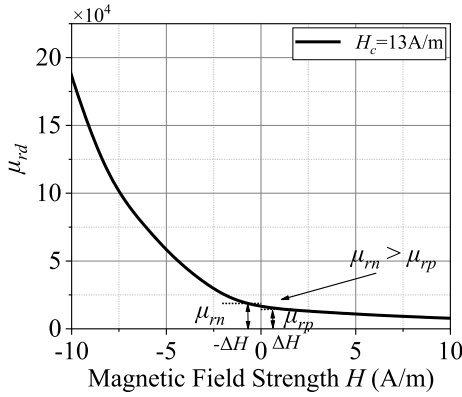


**FIGURE 2** Change trend of  $u_{rd}$  from  $B_s$  to  $B_r$  state of B30P105

When positive and negative DC voltages are applied, the positive and negative relative differential permeability ( $\mu_{rp}$  and  $\mu_{rm}$ ) can be expressed as

$$\begin{cases} \mu_{rp} = \frac{1}{\mu_0} \frac{\Delta B_p}{\Delta H} \\ \mu_{rm} = \frac{1}{\mu_0} \frac{\Delta B_n}{\Delta H} \end{cases} \quad (2)$$

where  $\Delta B_p$  and  $\Delta B_n$  represent the positive and negative change of flux density in the iron core, respectively.

In this work, a core formed by stacking silicon steel sheets of model B30P105 is selected as the analysis object. When the measurement frequency is 5 Hz, the hysteresis loops under ac excitation are obtained. To analyse  $\mu_{rd}$  change, its change trend from saturated flux density ( $B_s$ ) to the  $B_r$  state is shown in Figure 2. When  $H$  changes from positive to negative at  $B_r$ , the magnetization ability of the magnetic domain increases from small to large. If  $\Delta H$  is greater than 5% of the coercive force ( $H_c$ ), the difference between  $\mu_{rp}$  and  $\mu_{rm}$  is more obvious. It is expressed as

$$\mu_{rp} < \mu_{rm} \quad (3)$$

It is concluded that the direction of  $B_r$  is determined by comparing the values of  $\mu_{rp}$  and  $\mu_{rm}$ . However,  $\mu_{rp}$  and  $\mu_{rm}$  at

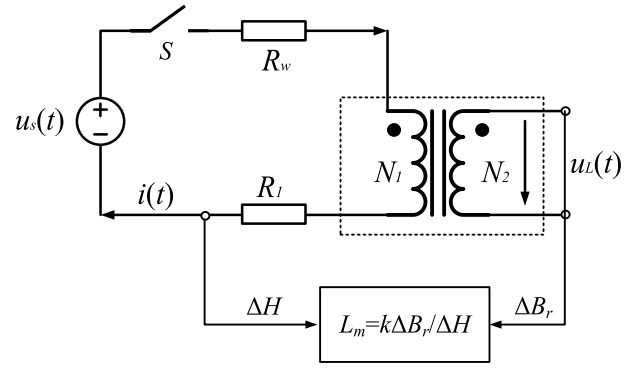


**FIGURE 3** DC measurement circuit of the proposed method

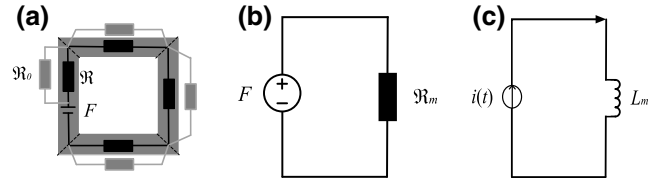


**FIGURE 4** (a) Magnetic circuit mode of the iron core. (b) Equivalent magnetic circuit of the iron core. (c) Equivalent circuit of the iron core

$B_r$  cannot be easily measured in actual measurement. It requires a measurable variable that can reflect the change of  $\mu_{rd}$ .

## 2.2 | Measurement circuit analysis of the proposed method

When positive and negative DC voltages are applied to one winding of the transformer, the magnetising inductance ( $L_m$ ) at  $B_r$  can be obtained by the measured respond current and induced voltage. If the positive DC voltage (same direction as initial  $B_r$ ) is applied, a positive magnetising inductance ( $L_p$ ) can be obtained. On the other hand, if the negative DC voltage (opposite direction as initial  $B_r$ ) is applied, a negative magnetising inductance ( $L_n$ ) can be obtained. Through magnetic circuit analysis,  $\mu_{rd}$  can be reflected by the  $L_m$  at  $B_r$ . Therefore,  $B_r$  in the iron core can be measured by analysing the relationship between  $B_r$  and  $L_p$  or  $L_n$ .

Figure 3 shows the DC measurement circuit of the proposed method. As shown,  $u_s(t)$  expresses the applied DC voltages (can be positive or negative).  $R_l$  and  $R_w$  stand for the limiting current resistance in the circuit and winding resistance, respectively. When  $u_s(t)$  is applied, the respond current  $i(t)$  and induced voltage  $u_L(t)$  can be measured in the circuit to obtain the magnetising inductance  $L_m$ . The square iron core is investigated in this work. The magnetic circuit and the circuit mode of the square iron core are shown in Figure 4. The magnetomotive force source on the winding side is denoted by  $F$ , and  $\mathfrak{R}$  corresponds to the reluctance through the legs and yokes.  $\mathfrak{R}_0$  represents the leakage path between the winding and the air. Since the core material

permeability is much larger than the air,  $\mathfrak{R}_0$  is much larger than the remaining reluctances in most cases so that it can be ignored, as shown in Figure 4b.  $\mathfrak{R}_m$  represents the equivalent reluctance of the core, which is expressed as

$$\mathfrak{R}_m = \frac{l}{\mu_0 \mu_{rd} S} \quad (4)$$

where  $S$  and  $l$  are the cross-sectional area and the average magnetic path length of the square core, respectively.

In a uniform magnetic field, according to Ohm's law for a magnetic circuit, the following equation is obtained:

$$F = N_1 i(t) = \mathfrak{R}_m \Phi(t) \quad (5)$$

where  $N_1$  is the turn number of transformer windings. When the DC voltage is applied,  $i(t)$  and  $\Phi(t)$  are the respond current and magnetic flux in the iron core with time.

When the DC voltage is applied, according to Equation (5), the following equation can be obtained:

$$\frac{di(t)}{dt} = \frac{\mathfrak{R}_m}{N_1} \frac{d\Phi(t)}{dt} \quad (6)$$

Based on the electromagnetic induction law,  $\Phi(t)$  is expressed as

$$\frac{d\Phi(t)}{dt} = \frac{L_m}{N_1} \frac{di(t)}{dt} \quad (7)$$

Based on Equations (1) and (4) to (7),  $L_m$  at  $B_r$  is expressed as

$$L_m = \frac{N_1^2}{\mathfrak{R}_m} = \frac{N_1^2 S}{l} \cdot \frac{\Delta B_r}{\Delta H} = k \cdot \frac{\Delta B_r}{\Delta H} \quad (8)$$

where  $k$  is the parameter associated with the core.

After the core parameters are determined, there is a proportional relationship between  $\mu_{rd}$  and  $L_m$ . According to Equations (3) and (8), the relation between  $L_p$  and  $L_n$  is expressed as

$$L_p < L_n \quad (9)$$

It shows that the direction of  $B_r$  can be determined by comparing the value of  $L_p$  and  $L_n$ .

The empirical formula for calculating residual flux density can be expressed as

$$B_r = f(L_m) \quad (10)$$

In the following sections, the empirical formula of the square core is obtained by FEM and its accuracy is proven by experiments.

### 3 | SIMULATION ANALYSIS

In this work, an experimental platform that adopts a square stacked steel sample is built and is shown in Section 4. The main dimension of the iron core is determined as  $S = 0.0016 \text{ m}^2$ ,  $l = 1.92 \text{ m}$ . To ensure the accuracy of the established finite element model, several key points need to be addressed, including the range of preset residual flux density, the measurement of local magnetic properties in the iron core, and the range of applied DC voltage.

#### 3.1 | Range of preset residual flux density

After the core is completely demagnetised, a larger DC excitation is first applied to the iron core to generate an  $H_1$ . As  $H_1$  increases, the flux density increases. Then, when the applied  $H_1$  is removed, due to the hysteresis characteristics of ferromagnetic materials, a preset  $B_r$  will be generated in the iron core. Under different  $H_1$ , the measured DC magnetization curve and preset  $B_r$  of the iron core are shown in Figure 5. As shown,  $B_s$  of the square core can reach 1.7 T. According to the empirical estimation method [5–7], the range of preset  $B_r$  is about 0.2–0.7 of  $B_s$ . Thus, the preset  $B_r$  is in the range of 0.34–1.19 T. There is a piecewise linear relationship between preset  $B_r$  and  $H_1$ , expressed as

$$\begin{cases} B_r = 0.0543H_1 + 0.0301 & 0.34T \leq B_r < 0.8T \\ B_r = 0.0016H_1 + 0.8163 & 0.8T < B_r \leq 1.19T \end{cases} \quad (11)$$

According to Equation (11),  $B_r$  can be preset more accurately. As long as the material properties are the same, the above relation can also be applied to the actual transformer core.

#### 3.2 | Measurement of local magnetic properties

Since the local magnetic properties at  $B_r$  are different from the magnetic properties of the core material, the local magnetic properties at  $B_r$  need to be measured in this study. The measurement progress of the local magnetic properties is shown in Figure 6. For each preset  $B_r$ , when different polarity dc voltage  $u_s(t)$  is applied to the transformer winding,  $i(t)$  and  $u_L(t)$  in Figure 3 can be measured. By repeating the above processing, the local magnetic properties at different  $B_r$  can be obtained. Based on the electromagnetic induction law and Ampere's law,  $\Delta B_r(t)$  and  $\Delta H(t)$  can be expressed as

$$\begin{cases} \Delta B_r(t) = \frac{1}{N_2 S} \cdot \int_0^t u_L(t) dt \\ \Delta H(t) = \frac{N_1}{l} \cdot i(t) \end{cases} \quad (12)$$

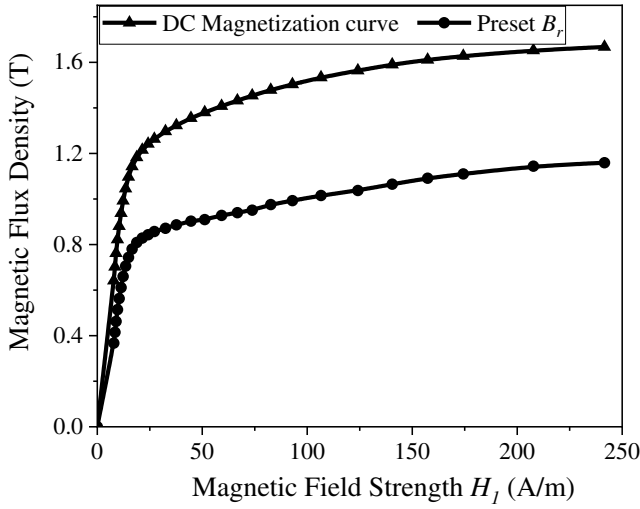


FIGURE 5 DC magnetization curve and preset  $B_r$  in the iron core

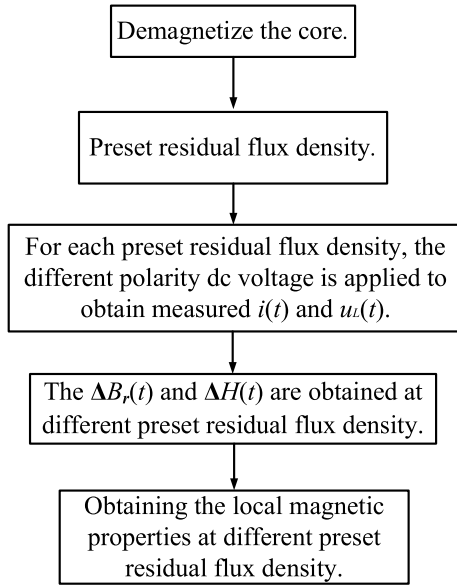


FIGURE 6 Measurement process of local magnetic properties

where  $N_1$  and  $N_2$  are the turn numbers of the primary and secondary windings, respectively.

Figure 7 shows the measured local BH curves when  $V_{dc}$  is 140 mV. As shown, by analysing the magnetization process of local BH curves, the relationship between  $B$  and  $H$  can be piecewise linearised, described by

$$B(H) = \begin{cases} k_0 H, & 0 < H \leq H_0 \\ k_1 H - (k_1 - k_0)H_0, & H_0 < H \end{cases} \quad (13)$$

where  $k_0$  is a constant independent of  $B_r$ , and its value is  $0.863 \times 10^{-3} \text{ T/m}$ .  $k_1$  is related to  $B_r$ , and  $k_1 > k_0$ .  $H_0$  is only related to the magnetic material and its value is the average value of  $H_1$  and  $H_2$ .  $H_0$  is 0.45 A/m. When  $H$  is greater than  $H_1$  or  $H_2$ , the magnetic flux density increases linearly with  $H$ . The local BH curves is mainly affected by the residual flux

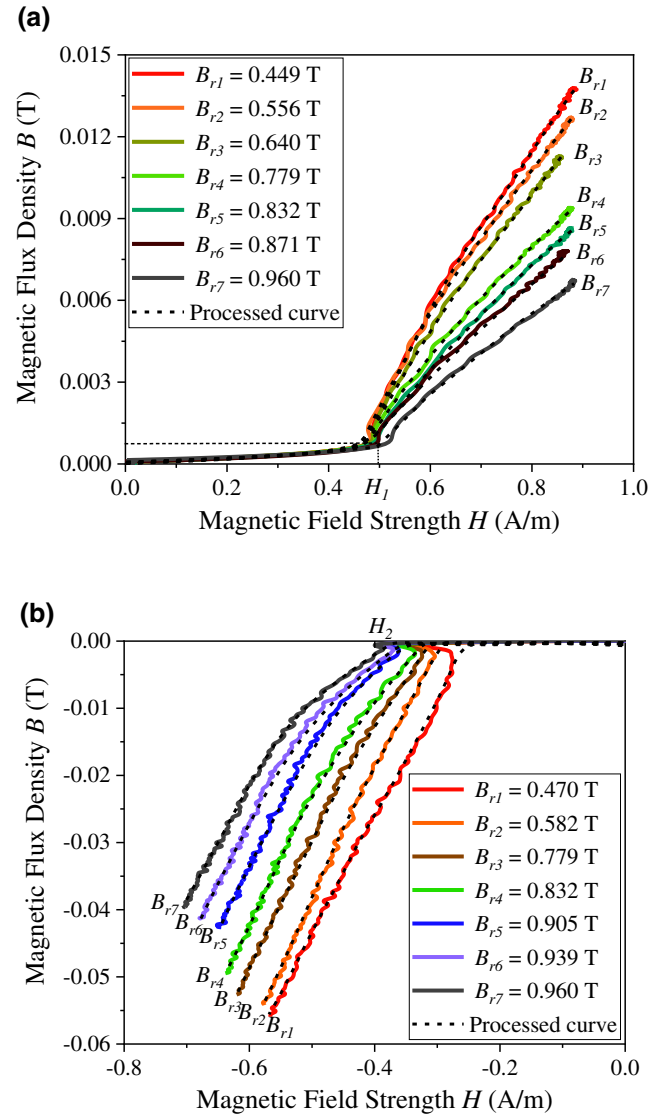
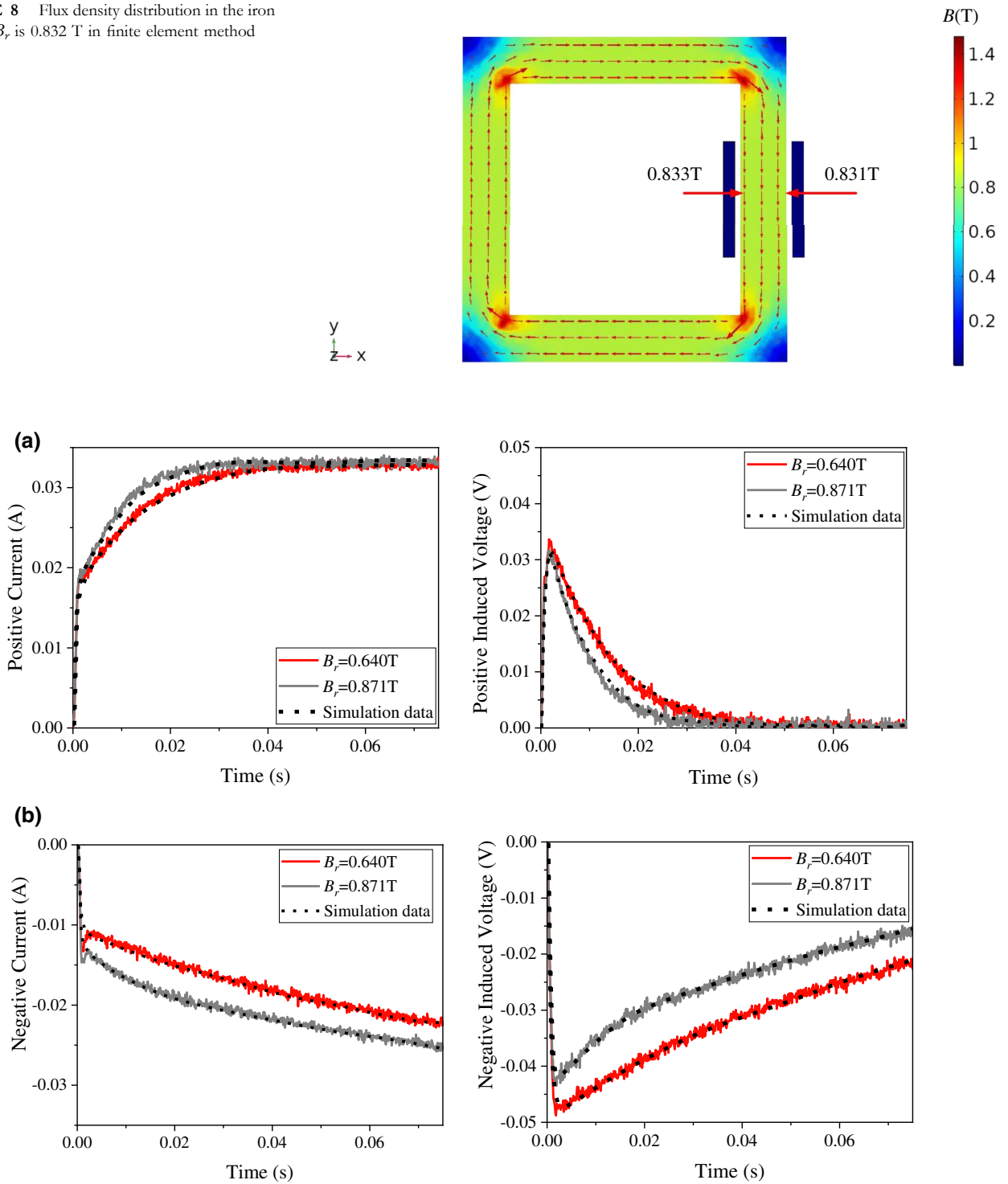


FIGURE 7 Local BH curves when  $V_{dc}$  is 140 mV. (a) Positive local BH curves. (b) Negative local BH curves

density in the iron core. After the local BH curves are set as the material properties of the core, the finite element model of the square core is established. When preset  $B_r$  is 0.832 T, the flux density distribution of the iron core in FEM is as shown in Figure 8. Since the length of the magnetic circuit inside the core is shorter than that on the outside, the flux density inside the core is higher than that on the outside. The relative errors between them and the average flux density are within 0.12%. Thus, the flux density mentioned in this work is the average flux density.

Figure 9 illustrates the measured respond current and induced voltage waveforms at different  $B_r$  with both positive and negative  $V_{dc}$ . As shown, when preset  $B_r$  is 0.64 T or 0.871 T, the measured current and induced voltage waveforms are in good agreement with the simulation waveforms, which proves the accuracy of the finite element simulation model.

**FIGURE 8** Flux density distribution in the iron core when  $B_r$  is 0.832 T in finite element method



**FIGURE 9** Waveforms of measured current and voltage when  $V_{dc}$  is applied. (a)  $V_{dc} = 140$  mV. (b)  $V_{dc} = -140$  mV

### 3.3 | Range of applied DC voltage

Figure 10 shows the local BH loops under different DC voltages when  $B_r$  is 0.64 and 0.871 T. As shown, under the same  $B_r$ , when different  $+V_{dc}$  is loaded, the local BH curves are parallel in the second stage. With the increase of  $V_{dc}$ , the slope of the local BH curves in the second stage is basically

unchanged. It shows that  $L_p$  at  $B_r$  is unchanged at different  $V_{dc}$ . However, when  $-V_{dc}$  is loaded, the local BH curves are different in the second stage. As  $V_{dc}$  increases, the slope of the local BH curves in the second stage varies with time. It shows that  $L_n$  is affected more when  $V_{dc}$  changes. Therefore, it is better to use  $L_p$ , rather than  $L_n$  as the independent variable to measure  $B_r$ .

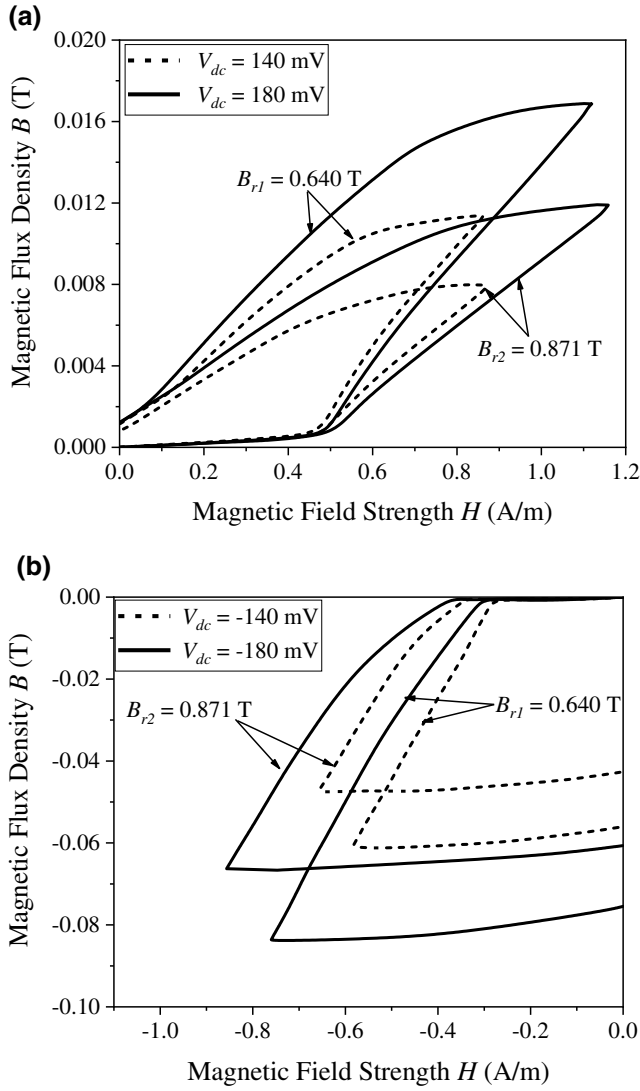


**FIGURE 10** Local BH loops at different DC voltages. (a) Positive local BH loops. (b) Negative local BH loops

To keep  $B_r$  from being changed too much, this work studies the range of  $V_{dc}$ . As shown in Figure 10b, as  $-V_{dc}$  increases, the change of  $B_r$  will be larger than that of the positive process. Thus, it is only necessary to analysis the change of  $\Delta B_n$  for determining the range of applied  $V_{dc}$ . When  $-V_{dc}$  is applied,  $i(t)$  and  $u_L(t)$  are expressed as

$$\begin{cases} i(t) = \frac{-V_{dc}}{R} \left(1 - e^{-\frac{t}{\tau_1}}\right) \\ u_L(t) = L_1 \frac{di(t)}{dt} \end{cases} \quad (14)$$

where  $\tau_1$  and  $L_1$  express the time constant and the magnetising inductance, respectively.

Based on the electromagnetic induction law, the change of flux density ( $\Delta B_1$ ) in the iron core is expressed as

$$\Delta B_1 = \frac{1}{N_2 S} \int_0^t u_L(t) dt = \frac{V_{dc} L_1}{N_2 S R} (1 - e^{-t/\tau_1}) \quad (15)$$

Similarly, when  $-V_{dc}$  is removed, the change of flux density ( $\Delta B_2$ ) is calculated by

$$\Delta B_2 = \frac{V_{dc} L_2}{N_2 S R} (1 - e^{-t/\tau_2}) \quad (16)$$

where  $\tau_2$  and  $L_2$  express the time constant and magnetising inductance, respectively.

In the negative voltage loading and removing process, the change of  $\Delta B_n$  is expressed as  $\Delta B_1 - \Delta B_2$ , which must be less than the change of initial  $B_r$ .

$$\frac{\Delta B_n}{B_r} = \frac{\Delta B_1 - \Delta B_2}{B_r} \leq \frac{\Delta B_r}{B_r} \quad (17)$$

Based on Equations (15) to (17),  $V_{dc}$  is expressed as

$$V_{dc} \leq \frac{\Delta B_r N_2 S R}{L_1 \left(1 - e^{-\frac{t}{\tau_1}}\right) - L_2 \left(1 - e^{-\frac{t}{\tau_2}}\right)} \quad (18)$$

To get the maximum value of applied  $V_{dc}$ , the above equation can be simplified to

$$V_{dcmax} \leq \frac{\Delta B_r N_2 S R}{L_1} \quad (19)$$

When  $-V_{dc}$  is loaded, the value of  $L_1$  is also  $L_n$ . Thus, the maximum value of  $V_{dc}$  is expressed as

$$V_{dcmax} \leq \frac{\Delta B_r N_2 S R}{L_n} \quad (20)$$

According to Ampere's loop law, when  $V_{dc}$  is applied, the following relation is obtained:

$$N_1 \cdot \frac{V_{dc}}{R} = H \cdot l \quad (21)$$

As shown in Figure 2, when  $H$  is not less than 5% of  $H_c$ , the difference between  $\mu_{rp}$  and  $\mu_{rm}$  is more obvious. Thus, the minimum value of  $V_{dc}$  is expressed as

$$V_{dcmin} \geq \frac{5\% H_c R l}{N_1} \quad (22)$$

Based on Equations (20) and (22), the range of  $V_{dc}$  is

$$\frac{5\% H_c R l}{N_1} \leq V_{dc} \leq \frac{\Delta B_r N_2 S R}{L_n} \quad (23)$$

**TABLE 1** Parameters of core and circuit

Core and circuit parameters	Value
Average magnetic circuit length of the iron core $l$	1.92 m
Cross-sectional area of the iron core $S$	0.0016 m <sup>2</sup>
The coercive force $H_c$	13 A/m
When $B_r$ is 0.36 T, the average of $L_n$ at different $V_{dc}$	0.3 H
Total resistance $R$	4.1 $\Omega$
The number of turns of measuring winding $N_1$	50
The number of turns of measuring winding $N_2$	25

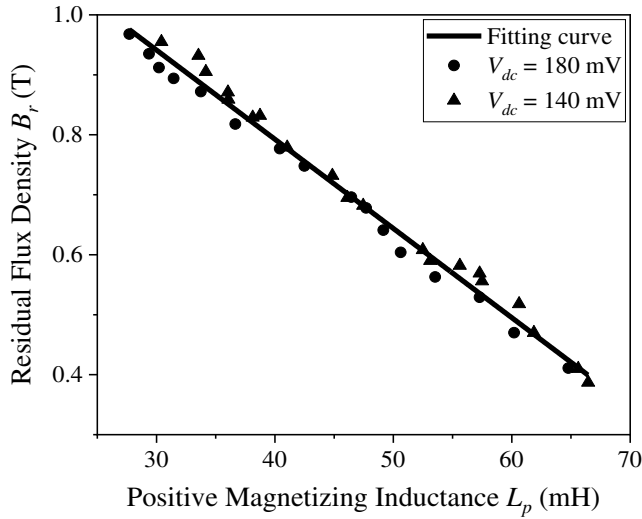
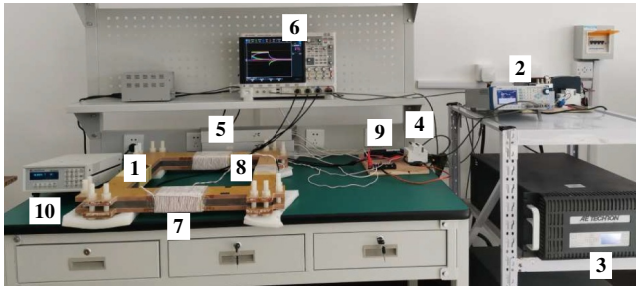
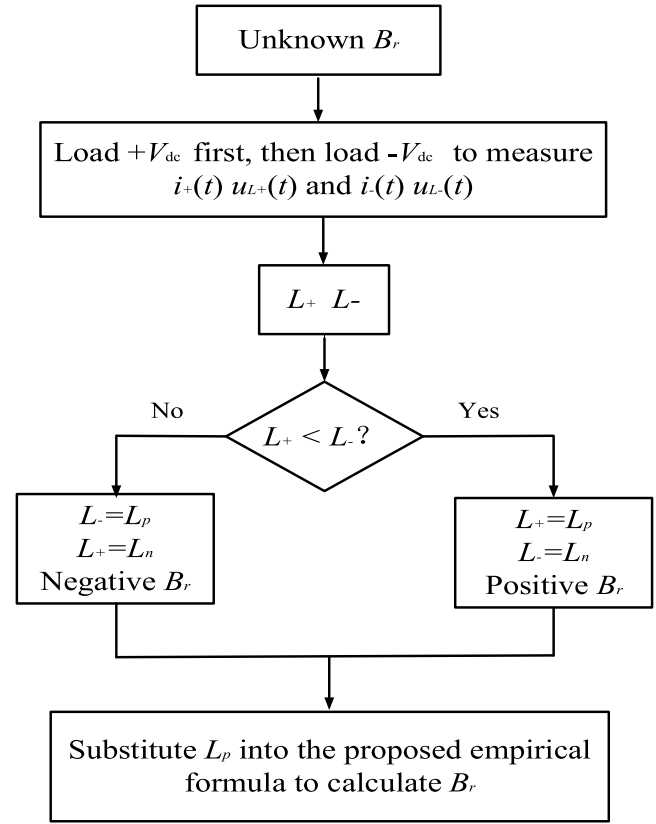
**FIGURE 11** Relation between  $B_r$  and  $L_p$  at different  $V_{dc}$ **FIGURE 12** Experimental platform of the proposed method. 1. Square core. 2. Signal generator. 3. Power amplifier. 4. Switch. 5. Series resistance. 6. Oscilloscope. 7. Primary winding. 8. Secondary winding. 9. Current probe. 10. Fluxmeter-480

Table 1 shows the parameters of the core and circuit. Submitting these parameters into Equation (23), the range of applied dc voltage can be obtained, expressed as

$$102 \text{ mV} \leq V_{dc} \leq 197 \text{ mV} \quad (24)$$

**FIGURE 13** Measurement process of the proposed method

### 3.4 | Empirical formula

When  $V_{dc}$  is applied,  $i(t)$  and  $u_L(t)$  are measured under different  $B_r$  to obtain the corresponding  $L_p$  values. Figure 11 illustrates the relation between  $B_r$  and  $L_p$  at different  $V_{dc}$ . By using the data fitting method, the empirical formula of the square core is expressed as

$$B_r = -0.0149L_p + 1.3876 \quad (25)$$

## 4 | EXPERIMENTAL RESULTS ANALYSIS

### 4.1 | Experimental platform

Figure 12 shows the experimental platform of the proposed method. As shown, the square core (item 1) adopts Baosteel's 0.3 mm silicon steel sheet. The model of this silicon steel sheet is B30P105. The width of each laminated core is 80 mm, and the thickness of the laminated core is 20 mm. The lamination factor of the iron core is 0.98. The inner and outer widths of the core are 400 and 560 mm, respectively. The signal generator

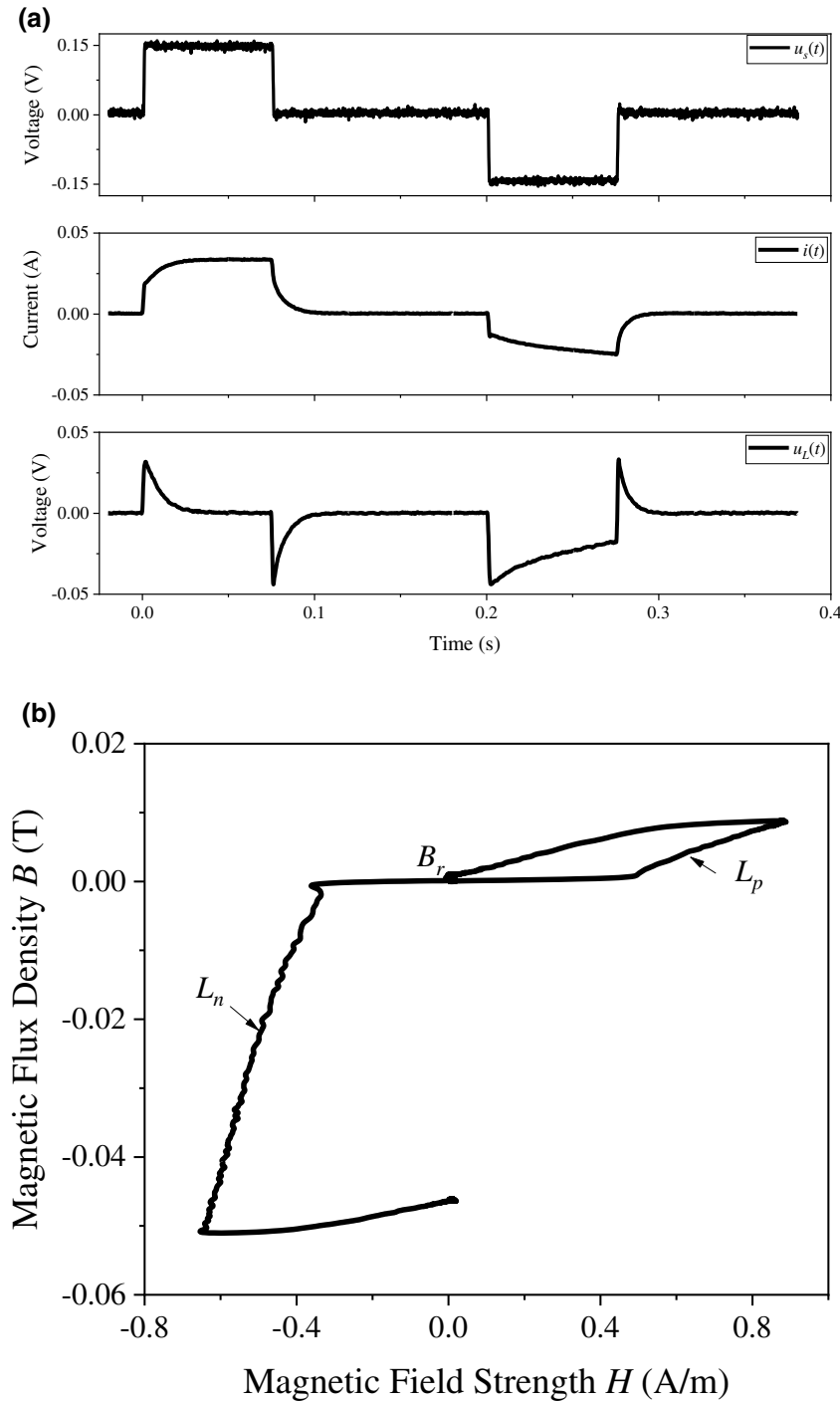


**FIGURE 14** Measured waveforms when  $B_r$  is 0.77 T and  $V_{dc}$  is 0.15 V. (a) Waveforms of applied DC voltage, respond current, and induced voltage. (b) Local BH hysteresis loops

(item 2) is used to generate positive and negative DC voltages signals, then amplified by the power amplifier (item 3) and finally applied to the DC measurement circuit. The generated DC voltages are expressed as  $+V_{dc}$  and  $-V_{dc}$ , respectively. The switch (item 4) can control the on-off in the measurement circuit and the series resistance (item 5) can limit the current flowing in the winding. When the DC voltage is applied, the oscilloscope (item 6) can be used to observe the respond current of primary winding (item 7) and the induced voltage of secondary winding (item 8). The current probe (item 9) is used

to collect the current signal flowing in the primary winding. The model of the current probe is N2782B, which can accurately measure currents at the ms or even  $\mu$ s level. Through the voltage integration principle, when the DC voltage is loaded, the real-time change of magnetic flux density can be tracked by using the Fluxmeter-480 (item 10).

Figure 13 shows the measurement process of the proposed method. After the transformer is powered off, the direction and magnitude of  $B_r$  is unknown. At this time, when  $+V_{dc}$  with the same polarity as  $B_r$  is first applied, the positive respond

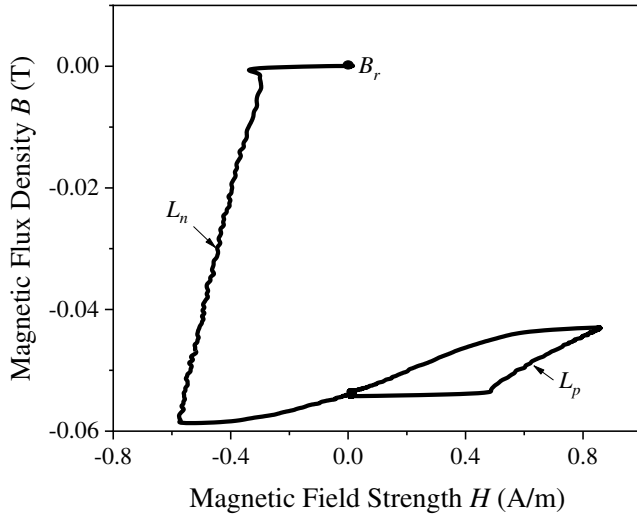


**FIGURE 15** Local BH hysteresis loops when  $B_r$  is  $-0.542$  T and  $V_{dc}$  is  $150$  mV

**TABLE 2** Experimental results of the proposed method

$B_r$ (T)	$L_p$ (mH)	$B_{rc}$ (T)	$B_{rv}$ (T)	$\varepsilon_1$ (%)	$\varepsilon_2$ (%)
0.410	64.74	0.423	0.360	3.17	12.20
0.592	52.32	0.608	0.530	2.70	10.47
0.690	45.61	0.708	0.625	2.61	9.42
0.950	28.43	0.964	0.860	1.47	9.47
1.020	24.13	1.028	0.920	0.78	9.80
-0.362	69.97	-0.345	0.310	4.70	14.37
-0.561	57.09	-0.537	0.503	4.28	10.34
-0.625	52.32	-0.608	0.560	2.72	10.40
-0.845	37.02	-0.836	0.765	1.07	9.47
-0.974	28.43	-0.964	0.890	1.03	8.62

current  $i_+(t)$  and induced voltage  $u_{L+}(t)$  can be measured. Then,  $L_+$  is obtained at  $B_r$ . When  $-V_{dc}$  is applied, the negative current  $i_-(t)$  and induced voltage  $u_{L-}(t)$  are measured, and  $L_-$  is obtained at  $B_r$ . On comparing the values of  $L_+$  and  $L_-$ , if  $L_+$  is less than  $L_-$ , it is determined that the smaller inductance value is  $L_p$  and the larger inductance value is  $L_n$ , so that it proves that the residual flux density in the core is positive  $B_r$ . If  $L_+$  is larger than  $L_-$ , the residual flux density in the core is negative  $B_r$ . Finally, the corresponding value of  $L_p$  is substituted into the proposed empirical formula to calculate  $B_r$  value in the core.

## 4.2 | Measurement of residual flux density

In the existing measurement methods, the voltage integration method is the most widely used and is a highly accurate magnetic flux measurement method. Therefore, this work compares the measurement error of the proposed method with

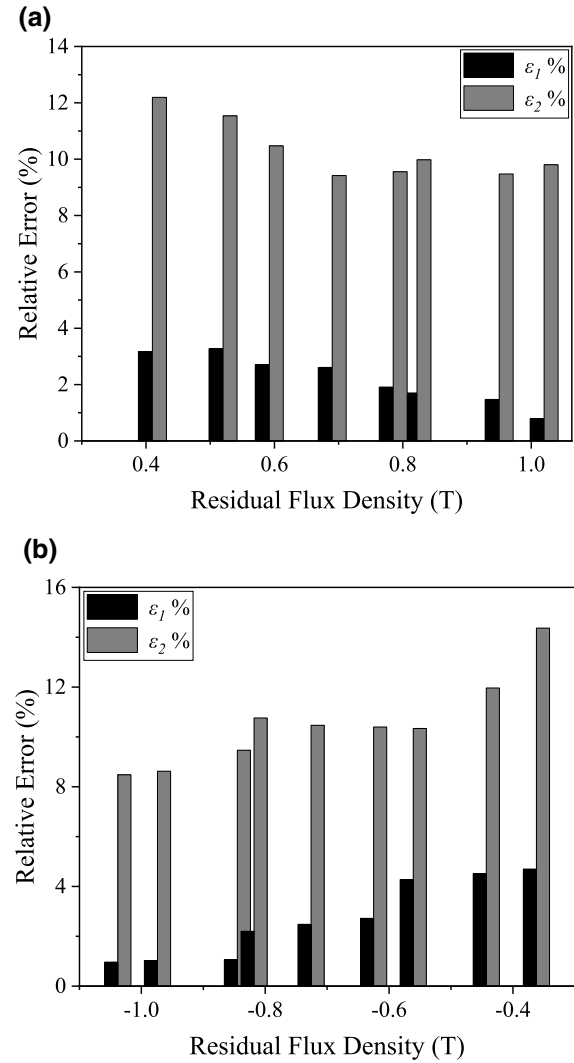


**FIGURE 16** Error comparison between proposed method and voltage integration method. (a) Positive  $B_r$ . (b) Negative  $B_r$

that of the voltage integration method to prove the accuracy of the proposed method. When dc voltage is applied,  $B_{rv}$  expresses the measured flux density by the voltage integration method, which can be observed by the Fluxmeter 480. The  $\varepsilon_1\%$  expresses the relative error between preset  $B_r$  and calculated residual flux density ( $B_{rc}$ ) by the proposed empirical formula. The  $\varepsilon_2\%$  expresses the relative error between preset  $B_r$  and  $B_{rv}$ .

$$\begin{cases} \varepsilon_1\% = \left| \frac{B_{rc} - B_r}{B_r} \right| \times 100\% \\ \varepsilon_2\% = \left| \frac{B_{rv} - B_r}{B_r} \right| \times 100\% \end{cases} \quad (26)$$

Figure 14 shows the measured waveforms when preset  $B_r$  is  $0.77$  T and  $V_{dc}$  is  $0.15$  V. As shown, when the positive and negative dc voltages are applied, the waveforms of response current and induced voltage are measured, and then the

corresponding local hysteresis loop is obtained in Figure 14b. It shows that in the second stage, the slope of the positive BH curve is 0.0195 and the slope of the negative BH curve is 0.181. Then,  $L_+$  and  $L_-$  are calculated as 40.62 and 377.02 mH. By comparison,  $L_+$  is less than  $L_-$ , so the direction of  $B_r$  can be judged. It is determined that the residual flux density in the iron core is positive  $B_r$ . The larger  $L_+$  is considered as  $L_p$ . After determining the  $B_r$  direction, the magnitude of  $B_r$  is calculated by the proposed empirical formula. Substituting  $L_p$  into the proposed empirical formula,  $B_r$  is calculated to be 0.782 T and  $\varepsilon_1\%$  is 1.56%.

When the transformer is powered off, the direction of  $B_r$  in the iron core is unknown. There will be a situation when the residual flux density in the iron core is a negative value. To verify the accuracy of the proposed method at  $-B_r$ , the local hysteresis loop is measured when preset  $B_r$  is  $-0.542$  T and  $V_{dc}$  is 0.15 V, as shown in Figure 15. It shows that after the load of the positive and negative DC voltages,  $L_p$  and  $L_n$  are calculated as 58.2 and 443.62 mH, respectively. By comparison,  $L_p$  is less than  $L_n$ , and thus the residual flux density in the iron core is negative  $B_r$ . Then, substituting  $L_p$  into the proposed empirical formula,  $B_r$  is calculated to be  $-0.52$  T and  $\varepsilon_1\%$  is 4.06%. Table 2 shows the experimental results of the proposed method under positive and negative  $B_r$ . The corresponding error comparison between the proposed method and the voltage integration method is shown in Figure 16. It shows that the range of  $\varepsilon_1\%$  is 0.78%–4.7%, and the range of  $\varepsilon_2\%$  is 8.62%–14.37%. By comparison,  $\varepsilon_1\%$  is less than  $\varepsilon_2\%$  at same  $B_r$ , which proves that the proposed method has higher accuracy than the voltage integration method. Besides, the results show that the error in smaller  $B_r$  is large. When  $B_r$  is small, the possibility of generating inrush current is small. When  $B_r$  is large, this possibility is very high. Due to the high accuracy of the proposed method in this case, it can avoid the inrush current to a large extent, which is very beneficial to the safe operation of the power grid. The direction of  $B_r$  has been determined. When the closing direction of the transformer is opposite to the polarity of measured  $B_r$ , no magnetising inrush current will be generated.

## 5 | CONCLUSION

This work presented an accurate residual flux density measurement method for power transformer cores based on magnetising inductance. The proposed method has several pros, including the following: (1) It does not need to know the past state of the transformer and is able to measure the residual flux density in the iron core by connecting the DC measurement circuit. (2) When positive and negative DC voltages are applied, the direction of residual flux density can be judged by comparing the values of positive and negative magnetising inductance. (3) The residual flux density is accurately calculated by the proposed empirical formula, and the maximal relative error is less than 5%. Compared with the voltage integration method, it has higher accuracy. This method also has several cons. To improve the accuracy of the finite element model, it is

necessary to measure the local magnetic properties in advance, which makes the extraction of empirical formulas difficult. Moreover, although many transformers share the same structure, there are still some uncertain factors that may affect their parameters and further study is needed.

In this research, the local magnetic properties are different from the magnetic properties of iron core materials. It is inaccurate to directly use the magnetic properties of iron core materials to study residual flux in the existing research. If we want to measure residual flux more accurately, we can consider introducing a local hysteresis model. To further improve the applicability of the empirical formula, the proposed method will be applied to the actual single-phase transformer with the same structure and material. Subsequently, this method will be extended to three-phase transformers.

## ACKNOWLEDGEMENTS

This work was supported by the National Natural Science Foundation of China under Grant 51877065 and Science and Technology Research Project of Higher Education Institutions in Hebei Province of China under Grant QN2016200.

## CONFLICT OF INTEREST

We declare that we have no conflict of interest.

## DATA AVAILABILITY STATEMENT

The data that support the findings of this study are available from the corresponding author upon reasonable request.

## ORCID

Cailing Huo  <https://orcid.org/0000-0001-5480-2007>

## REFERENCES

1. Rezaeaealam, B., et al.: Impacts of ferroresonance and inrush current forces on transformer windings. *IET Electr. Power Appl.* 13(7), 1–5 (2019)
2. Mitra, J., et al.: Reduction of three-phase transformer inrush currents using controlled switching. *IEEE Trans. Ind. Appl.* 56(1), 890–897 (2020)
3. De León, F., et al.: Elimination of residual flux in transformers by the application of an alternating polarity DC voltage source. *IEEE Trans. Power Del.* 30(4), 1727–1734 (2015)
4. Zhang, S., et al.: Improved flux-controlled VFCV strategy for eliminating and measuring the residual flux of three-phase transformers. *IEEE Trans. Power Del.* 35(3), 1237–1248 (2020)
5. Santagostino, E.C.G.: Results of the enquiries on actual network conditions when switching magnetizing and small inductive currents and on transformer and shunt reactor saturation characteristics. *Electra*. 94, 35–53 (1984)
6. Brunke, J.H., Frohlich, K.J.: Elimination of transformer inrush currents by controlled switching. I. Theoretical considerations. *IEEE Trans. Power Del.* 16(2), 276–280 (2001)
7. Wu, Y.: Research on no-load test of 1000kv ultra-high voltage transformer. In: 2011 Asia-Pacific Power and Energy Engineering Conference, pp. 1–6. (2011)
8. Wang, K.: Research on residual flux characteristics of transformer with single-phase four-limb core under different DC excitation current. In: 2020 IEEE International Conference on High Voltage Engineering and Application (ICHVE), pp. 1–5. Beijing (2020)
9. Taylor, D.I.: Single-phase transformer inrush current reduction using pre-fluxing. *IEEE Trans. Power Del.* 27(1), 245–252 (2021)
10. Wang, Z.B., Liang, H.: Analysis and research of pre-magnetizing transformer. *Transformers*. 58(3), 32–35 (2021)

11. Liu, T.: Remaining flux measurement method of ferromagnetic element core based on polarity variation DC voltage source. *Trans. China Electrotech. Soc.* 32(13), 137–144 (2017)
12. Hodgdon, M.L.: Applications of a theory of ferromagnetic hysteresis. *IEEE Trans. Magn.* 24(1), 218–221 (1988)
13. Takajo, S., et al.: Effect of silicon content on iron loss and magnetic domain structure of grain-oriented electrical steel sheet. *IEEE Trans. Magn.* 54(1), 1–6 (2018)
14. Fang, S., et al.: A novel strategy for reducing inrush current of three-phase transformer considering residual flux. *IEEE Trans. Ind. Electron.* 63(7), 4442–4451 (2016)
15. Himata, Y., et al.: Residual magnetic flux of on-load transformer for controlled switching. *IEEJ Trans. Electr. Electron. Eng.* 15(8), 1134–1138 (2020)
16. Yong, L., et al.: Research on remaining magnetic measurement method of power transformer. *Power Syst. Protect. Cont.* 47(15), 1–6 (2019)
17. Zheng, T., Wang, Y.: Fast and in situ remanent flux detection method for a protection current transformer based on the fluxgate theory. *AIP Adv.* 11(1), 015–034 (2021)
18. Cavallera, D., et al.: A new method to evaluate residual flux thanks to leakage flux, application to a transformer. *IEEE Trans. Magn.* 50(2), 1005–1008 (2014)
19. Vulin, D., Milicevic, K., Petrovic, G.: Determining the residual magnetic flux value of a single-phase transformer using a minor hysteresis loop. *IEEE Trans. Power Del* (2020)
20. Wenqi, G., et al.: Residual flux in the closed magnetic core of a power transformer. *IEEE Trans. Appl. Supercond.* 24(3), 1–4 (2014)
21. Huo, C., et al.: Residual flux measurement of the single-phase transformer based on transient current method. *IEEE Trans. Appl. Supercond.* 30(4), 1–5 (2020)

**How to cite this article:** Huo, C., et al.: Study on the residual flux density measurement method for power transformer cores based on magnetising inductance. *IET Electr. Power Appl.* 16(2), 224–235 (2022). <https://doi.org/10.1049/elp2.12148>